

Microscopic Study of Ionic Liquid–H₂O Systems: Alkyl-Group Dependence of 1-Alkyl-3-Methylimidazolium Cation

Takashi Masaki, Keiko Nishikawa, and Hideaki Shiota*

Department of Nanomaterial Science, Graduate School of Advanced Integration Science, Chiba University, 1-33 Yayoi, Inage-ku, Chiba 263-8522, Japan

Received: February 28, 2010; Revised Manuscript Received: April 11, 2010

We have investigated the microscopic aspects for ionic liquid–H₂O systems by Raman and IR spectroscopies. Ionic liquids studied here are a series of 1-alkyl-3-methylimidazolium cations (alkyl groups: ethyl, butyl, hexyl, octyl, and decyl groups) with the anions of tetrafluoroborate and bis(trifluoromethanesulfonyl)amide. Polarities of the ionic liquid–H₂O systems have also been measured by means of a solvatochromic dye, betaine 33. Vibrational bands of the anions shift to the higher frequency with the higher water content. We have also found that the magnitude of the frequency shifts of the anions' vibrational modes by adding water becomes smaller with the longer alkyl group of cation. From the comparison of the vibrational spectroscopic result with the result of the solvatochromic experiment, it has become clear that the frequency shift of the vibrational modes of anions almost correlates with the polarity. On the other hand, the feature of the vibrational band of water stretching mode is not really changed among the cations with the different alkyl groups. This evidence implies that the water aggregations localize at ionic regions and the water state does not really depend on the alkyl group of cation.

1. Introduction

Room-temperature ionic liquids (ILs) are molten salts at room temperature. One of the most unique natures of ILs is their low melting points. When the melting points of ILs are compared to those of crystalline salts (e.g., NaCl: 801 °C), the melting points of ILs are obviously low for salts. ILs are also unique liquids, because ILs show negligible vapor pressure at ambient standard conditions. Both the basic and application studies of the unique liquids/salts, room-temperature ILs, have become more active and extensive in these ten years.^{1–9}

One of the biggest issues on ILs is water as an impurity.^{1,10} Because ILs are ionic in nature, most ILs are hygroscopic and it is difficult to completely remove water from ILs. Physical properties of ILs are significantly changed by the existence of water, since water largely affects the interionic interaction in ILs.^{11–16} Therefore, it is important to understand the details of the interionic and ion–water interactions at the molecular-level aspect.

To understand the unique natures of ILs at microscopic perspective, vibrational spectroscopies have been widely used.^{17–24} Besides neat ILs, IL–H₂O systems were also investigated.^{25–32} Cammarata et al. studied the water state in imidazolium-based ILs with several anions and found that the state of water in ILs was greatly dependent on the anion.²⁵ Jeon et al. studied the water content dependence of the microscopic structure in 1-butyl-3-methylimidazolium tetrafluoroborate ([C₄MIm][BF₄])²⁶ and found that the intermolecular/interionic structure in the IL–H₂O system changed at the water concentrations of about 32 mol/L and 45 mol/L. They also measured [C₄MIm]I–H₂O system.²⁷ Danten et al. investigated the interaction of water highly diluted in 1-alkyl-3-methylimidazolium ILs with the anions of [BF₄][–] and [PF₆][–] by Raman and IR spectroscopies together with the *ab initio* quantum chemistry calculations.²⁸ This study

indicated that a monodispersed water molecule in the ILs formed a nearly symmetric structure of A···H–O–H···A (A: anion) via hydrogen bonds. Umebayashi et al. reported the pressure dependence study of some IL–H₂O mixtures²⁹ and found that the ionic association between water and imidazolium cation varies with different pressure conditions. Ludwig and co-workers showed a correlation between the vibrational frequencies of stretching modes of water and dielectric constants in IL–H₂O mixtures together with conventional solvents.³⁰

By time-resolved vibrational spectroscopy, Owrutsky and co-workers studied the frequency shift and relaxation time of antisymmetric stretching mode of azide (probe ion) in [C₄MIm][BF₄]-H₂O system.³¹ The result showed that the system was rather homogeneous in the entire concentration range. Koberga et al. measured the dielectric responses at terahertz region for [C₄MIm][BF₄]-H₂O systems by terahertz time-domain spectroscopy.³² They showed a nonlinearity in the relation between the concentration and relaxation times in the mixtures that were pronounced in the IL concentration between 40 and 90 vol %.

In this study, we focus on the alkyl-group dependence of 1-alkyl-3-methylimidazolium cation on the microstructure in IL–H₂O systems. It is understood that the physical properties such as shear viscosity, density, and melting point of 1-alkyl-3-methylimidazolium ([C_nMIm]⁺; *n* is the number of carbons of alkyl group) based ILs depend on the alkyl group of [C_nMIm]⁺ cation.^{1,33,34} However, there is no systematic report on the alkyl-group dependence of cation on the microscopic aspect in IL–H₂O systems. Here, we have chosen [C_nMIm]⁺ based ILs with two typical anions ([BF₄][–] and bis(trifluoromethylsulfonyl)amide: [NTf₂][–]) (Figure 1). We find in this study that the water aggregation state in the ILs is mainly determined by the ionic property in the ILs and is little influenced by the hydrophobicity of the ILs. However, the frequencies of the vibrational bands of [BF₄][–] and [NTf₂][–] in the ILs depend on

* E-mail: shiota@faculty.chiba-u.jp.

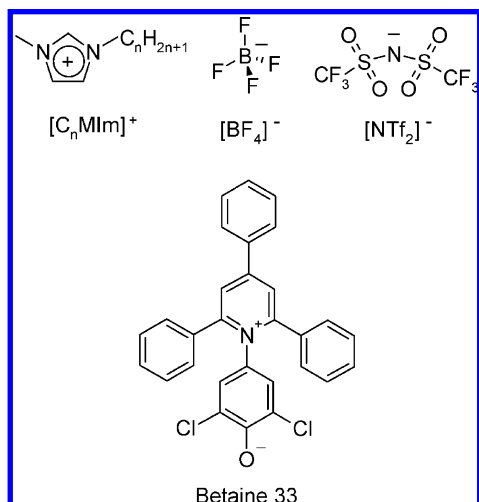


Figure 1. Structural formulas of cations and anions for the sample ionic liquids are shown. Structural formula of betaine 33 is also shown.

the water content. We will show the correlation between the frequency shifts of the vibrational bands of $[\text{BF}_4]^-$ and $[\text{NTf}_2]^-$ and the polarity probed by a solvatochromic probe, betaine 33.

2. Experimental Methods and Quantum Chemistry Calculations

$[\text{C}_2\text{Mim}][\text{NTf}_2]$, $[\text{C}_4\text{Mim}][\text{NTf}_2]$, and $[\text{C}_2\text{Mim}][\text{BF}_4]$ were obtained from Kanto Chemicals and used without further purification. H_2O (HPLC grade, Wako), D_2O (99.96D%, Aldrich), ethylene glycol (EG) (Wako), and betaine 33 (Figure 1, Fluka) were also used as received. $[\text{C}_4\text{Mim}][\text{BF}_4]$, $[\text{C}_6\text{Mim}][\text{BF}_4]$, $[\text{C}_8\text{Mim}][\text{BF}_4]$, $[\text{C}_{10}\text{Mim}][\text{BF}_4]$, $[\text{C}_6\text{Mim}][\text{NTf}_2]$, $[\text{C}_8\text{Mim}][\text{NTf}_2]$, and $[\text{C}_{10}\text{Mim}][\text{NTf}_2]$ were prepared according to the standard methods.^{34–37} The ILs were dried in vacuo (about 10^{-3} Torr) at 323 K over 48 h. All the products were identified by ^1H NMR and elemental analysis. Water contents of all the ILs were estimated by Karl Fischer titration using a Mettler Toledo Karl Fischer Coulometer (model DL32) and were below 500 ppm. Details of the synthesis procedures are summarized in Supporting Information.

IR spectra of the ILs and IL– H_2O mixtures were measured with a Jasco FT-IR spectrometer (FT/IR-6100) based on the attenuated total reflectance (ATR) method. Refractive indices based on a fluorescent lamp (Supporting Information) for the ILs and water were measured by a simplified refractometer (Atago, R-5000) to calibrate the refractive index that influences the distance from the boundary of the evanescent wave for ATR-IR measurements. The refractive index of water measured here was 1.333 that was identical with n_D of water (1.33336) at 293 K.³⁸ Raman spectra of the ILs and IL– H_2O mixtures were recorded with a Raman spectrometer (Kaiser Optical Systems, HoloLab 5000). The light source was a 785 nm diode laser, and the output power was 400 mW. Steady-state absorption spectrum measurements of betaine 33 in the samples were made with a Hitachi spectrophotometer (U-3900H). All the measurements were carried out at 298 ± 2 K.

Ab initio quantum chemistry calculations based on the B3LYP/6-311+G(d,p) level^{39,40} were performed to obtain the optimized structures and normal modes for $[\text{C}_2\text{Mim}][\text{BF}_4]$, $[\text{C}_2\text{Mim}][\text{BF}_4] \cdot \text{H}_2\text{O}$, and $[\text{C}_2\text{Mim}][\text{BF}_4] \cdot 2\text{H}_2\text{O}$ clusters by the Gaussian 03 program package.⁴¹ The atom coordinates are summarized in Supporting Information.

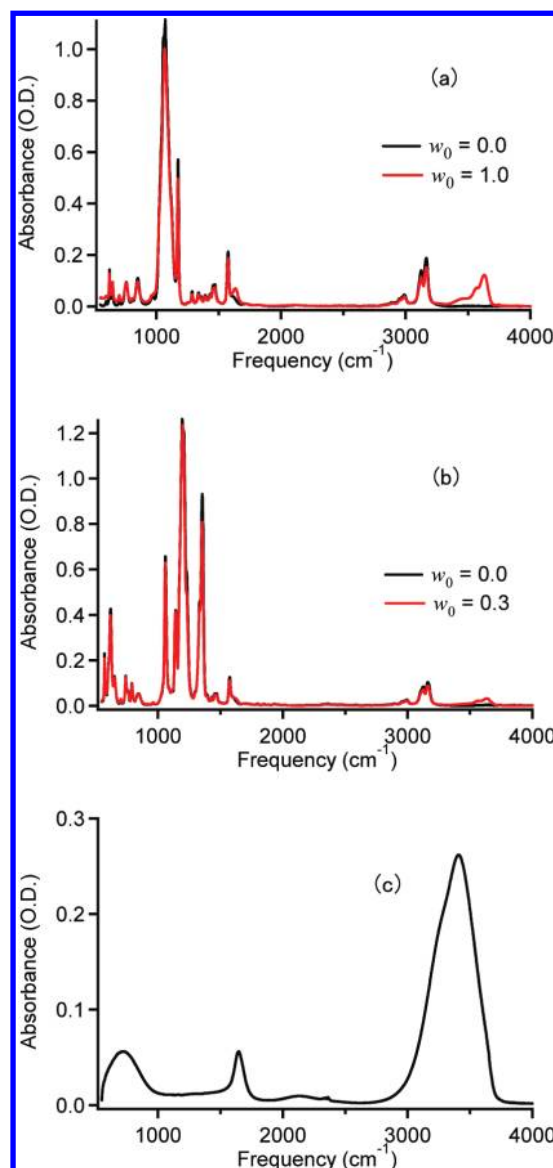


Figure 2. IR spectra of (a) neat $[\text{C}_2\text{Mim}][\text{BF}_4]$ (black) and $[\text{C}_2\text{Mim}][\text{BF}_4] \cdot \text{H}_2\text{O}$ with $w_0 = 1.0$ (red), (b) neat $[\text{C}_2\text{Mim}][\text{NTf}_2]$ (black) and $[\text{C}_2\text{Mim}][\text{NTf}_2] \cdot \text{H}_2\text{O}$ with $w_0 = 0.3$ (red), and (c) neat H_2O .

3. Results

3.1. Vibrational Spectra. 3.1.1. Vibrational Bands of Water. Figure 2 shows the IR spectra in $550\text{--}4000\text{ cm}^{-1}$ for (a) neat $[\text{C}_2\text{Mim}][\text{BF}_4]$ and $[\text{C}_2\text{Mim}][\text{BF}_4] \cdot \text{H}_2\text{O}$ with $w_0 (\equiv [\text{H}_2\text{O}]/[\text{IL}]) = 1.0$, (b) neat $[\text{C}_2\text{Mim}][\text{NTf}_2]$ and $[\text{C}_2\text{Mim}][\text{NTf}_2] \cdot \text{H}_2\text{O}$ with $w_0 = 0.3$ (water saturation concentration), and (c) neat water. Vibration bands at ca. 720, 1640, and 3400 cm^{-1} of water are libration, bending, and stretching modes, respectively.⁴² A low-intensity vibration band at about 2130 cm^{-1} is a water association band or a combination band of the libration and bending modes.⁴³ From a comparison between the neat $[\text{C}_2\text{Mim}][\text{BF}_4]$ and $[\text{C}_2\text{Mim}][\text{BF}_4] \cdot \text{H}_2\text{O}$, it is clear that water bands appear in the $[\text{C}_2\text{Mim}][\text{BF}_4] \cdot \text{H}_2\text{O}$. Although the intensities of water bands are low, they are also confirmed in the $[\text{C}_2\text{Mim}][\text{NTf}_2] \cdot \text{H}_2\text{O}$. In below, we will see the water content dependence of the vibrational bands of water with expanded view.

Figure 3 shows the IR spectra in $3000\text{--}3900\text{ cm}^{-1}$ of (a) $[\text{C}_2\text{Mim}][\text{BF}_4] \cdot \text{H}_2\text{O}$ and (b) $[\text{C}_{10}\text{Mim}][\text{BF}_4] \cdot \text{H}_2\text{O}$ mixtures with $w_0 = 0.0$ (neat ILs), 0.5, 1.5, and 2.5. In the low water

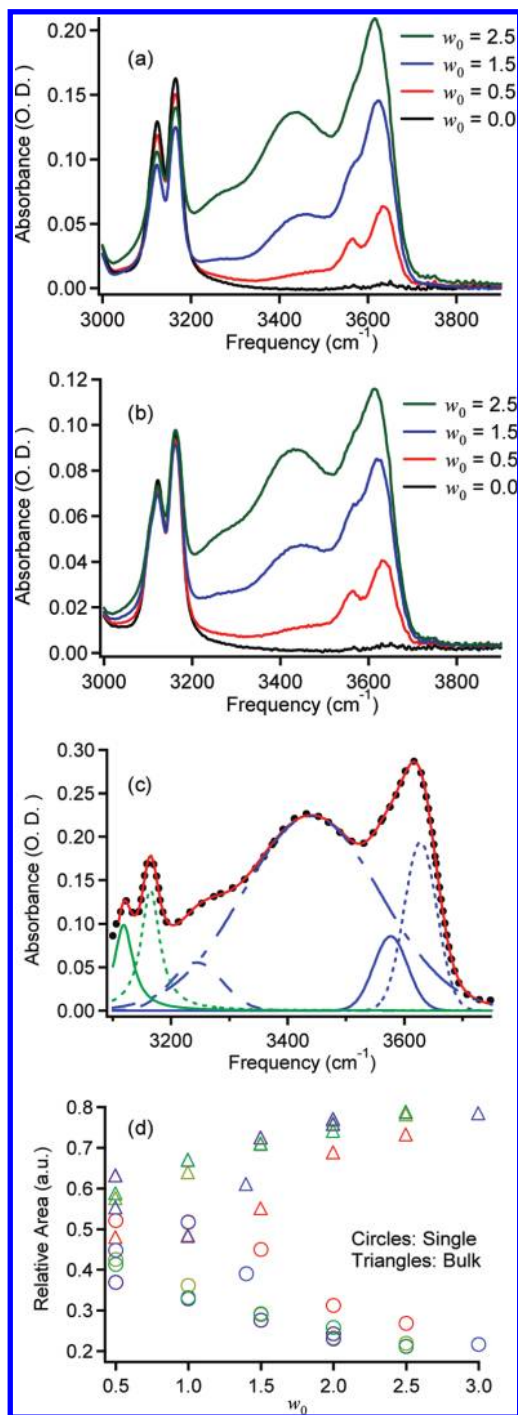


Figure 3. IR spectra of (a) neat [C₂MIm][BF₄] (black) and [C₂MIm][BF₄]-H₂O mixtures with $w_0 = 0.5$ (red), 1.5 (blue), and 2.5 (green); (b) neat [C₁₀MIm][BF₄] (black) and [C₂MIm][BF₄]-H₂O mixtures with $w_0 = 0.5$ (red), 1.5 (blue), and 2.5 (green). (c) IR spectrum (black dots) and its fit (red line) for [C₂MIm][BF₄]-H₂O mixture with $w_0 = 0.5$. Gauss functions (blue lines) are for the water's modes (modes at ca. 3250 and 3450 cm⁻¹ are for bulk water and modes at ca. 3560 and 3640 cm⁻¹ are for isolated water), and Lorentz functions (green lines) are for the cation's modes. (d) Plots of the relative areas, which are normalized to be 1 for the sum of the four bands' areas, of the isolated (3560 and 3640 cm⁻¹) and bulk water bands (3250 and 3500 cm⁻¹) vs w_0 for [C_nMIm][BF₄]-H₂O systems. Red, blue, green, yellow, and purple denote [C₂MIm][BF₄], [C₄MIm][BF₄], [C₆MIm][BF₄], [C₈MIm][BF₄], and [C₁₀MIm][BF₄] systems, respectively.

content region ($w_0 < 0.5$), two clear vibrational bands are observed at ca. 3560 and 3640 cm⁻¹. The 3560 and 3640 cm⁻¹ modes have been assigned as antisymmetric and symmetric stretching modes of isolated water molecules.^{25,44,45} These modes

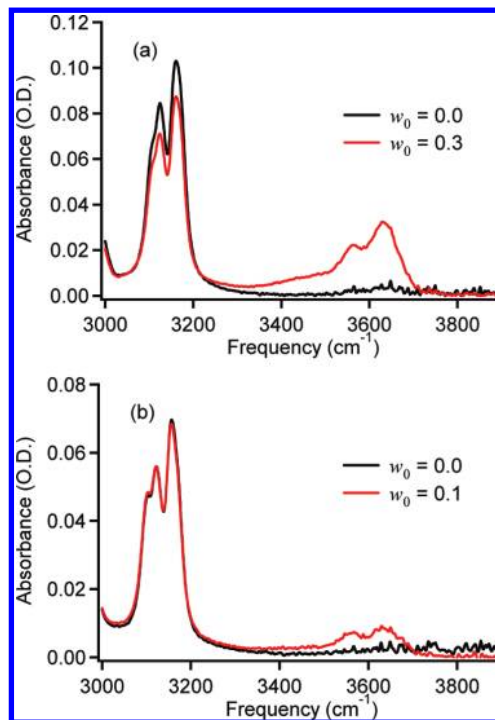


Figure 4. IR spectra of (a) neat [C₂MIm][NTf₂] (black) and [C₂MIm][NTf₂]-H₂O with $w_0 = 0.3$ (red) and (b) neat [C₁₀MIm][NTf₂] (black) and [C₁₀MIm][NTf₂]-H₂O with $w_0 = 0.1$ (red).

are sensitive to the environment. For example, these modes of water in vapor locate at 3656.7 and 3755.8 cm⁻¹,⁴⁴ and those in [C₄MIm][PF₆] locate at ca. 3600 and 3680 cm⁻¹.²⁸ The present result is in good agreement with the result in [C₄MIm][BF₄] reported by Danten, et al.²⁸ In $w_0 > 0.5$, two broad bands at ca. 3250 and 3450 cm⁻¹ become clear. Both the bands are due to hydrogen-bonded water. The former vibrational band (ca. 3250 cm⁻¹) is attributed to molecules in more regular structure with unstrained hydrogen bond (also observed in ice I form) and the latter band (ca. 3450 cm⁻¹) is due to water molecules in more distorted structures with energetically unfavored hydrogen bonds.^{42,46,47} As seen in Figure 3a and b, a clear difference in the vibrational spectra between [C₂MIm][BF₄]-H₂O and [C₁₀MIm][BF₄]-H₂O systems has not been confirmed. The IR spectra of the other [C_nMIm][BF₄]-H₂O systems studied here are also similar.

Spectral decomposition analysis was performed to determine the w_0 dependence of the ratio of isolated water and bulk water. A sum of four antisymmetrized Gaussian and two Lorentzian functions was used here. The former functions are for water's bands (ca. 3250, 3450, 3560, and 3640 cm⁻¹) and latter functions (ca. 3120 and 3165 cm⁻¹) are for the cation's bands. Figure 3c shows the IR spectrum and the fit for [C₄MIm][BF₄]-H₂O ($w_0 = 3.0$), as an example. Figure 3d plots the relative areas, which are normalized to be 1 for the sum of the four bands' areas, of the isolated (3560 and 3640 cm⁻¹) and bulk water bands (3250 and 3450 cm⁻¹) vs w_0 . The relative area of the isolated water's bands decreases and that of the bulk water's bands increases with increasing w_0 .

Figure 4 shows the IR spectra in 3000–3900 cm⁻¹ for (a) [C₂MIm][NTf₂]-H₂O ($w_0 = 0.0$ and 0.3) and (b) [C₁₀MIm][NTf₂]-H₂O ($w_0 = 0.0$ and 0.1). Because of the hydrophobic nature of [C_nMIm][NTf₂], only low water content mixtures are available (Table 1). Although the water content of the mixtures is low, the clear broad vibrational band is observed at ca. 3430 cm⁻¹.

TABLE 1: Formula Weights FW of $[C_n\text{MIm}][\text{BF}_4]$ and $[C_n\text{MIm}][\text{NTf}_2]$ ILs, Absorption Maxima λ_{max} of Betaine 33 in ILs, $E_T(33)$, Refractive Indices n , Water Saturation Vales S_w , and Molar Concentration Ratio between IL and Water at Water Saturation $w_{0\text{sw}}$ of ILs

IL	FW (g/mol)	λ_{max} (nm)	$E_T(33)$ (kcal/mol)	n	S_w (ppm)	$w_{0\text{sw}}$
$[\text{C}_2\text{MIm}][\text{BF}_4]$	197.97	460.9	62.03	1.409	-	-
$[\text{C}_4\text{MIm}][\text{BF}_4]$	226.02	464.5	61.55	1.420	-	-
$[\text{C}_6\text{MIm}][\text{BF}_4]$	254.08	465.3	61.45	1.426	171600	3.566
$[\text{C}_8\text{MIm}][\text{BF}_4]$	282.13	464.7	61.53	1.431	155900	2.892
$[\text{C}_{10}\text{MIm}][\text{BF}_4]$	310.18	464.6	61.54	1.434	141000	2.825
$[\text{C}_2\text{MIm}][\text{NTf}_2]$	391.31	469.2	60.93	1.421	14000	0.308
$[\text{C}_4\text{MIm}][\text{NTf}_2]$	419.37	470.2	60.81	1.427	11240	0.265
$[\text{C}_6\text{MIm}][\text{NTf}_2]$	447.42	468.4	61.04	1.431	7918	0.198
$[\text{C}_8\text{MIm}][\text{NTf}_2]$	475.47	473.6	60.37	1.434	5293	0.140
$[\text{C}_{10}\text{MIm}][\text{NTf}_2]$	503.53	474.2	60.29	1.436	3309	0.093

3.1.2. Vibrational Band of $[\text{BF}_4]^-$. Figure 5a shows the Raman spectra in 750–780 cm^{-1} for $[\text{C}_2\text{MIm}][\text{BF}_4]$ –H₂O system with $w_0 = 0.0$ (neat), 0.5, 1.0, 1.5, 2.0, and 2.5. The vibrational band is the symmetric F–B stretching mode of $[\text{BF}_4]^-$. We focus on this band to see the w_0 dependence of the vibrational frequency, because the band has a strong intensity and does not overlap with other vibrational bands. The vibrational band of $[\text{BF}_4]^-$ shifts to the high-frequency side with increasing w_0 . This feature has also been confirmed in the other $[\text{C}_n\text{MIm}][\text{BF}_4]$ ILs. Plots of the peak frequency of the vibrational mode vs w_0 in the $[\text{C}_n\text{MIm}][\text{BF}_4]$ –H₂O systems are shown in Figure 5b. The magnitude of the frequency shift becomes larger with the shorter alkyl group of cation.

3.1.3. Vibrational Band of $[\text{NTf}_2]^-$. The Raman spectra in 725–765 cm^{-1} of neat $[\text{C}_2\text{MIm}][\text{NTf}_2]$ and $[\text{C}_2\text{MIm}][\text{NTf}_2]$ –H₂O mixture ($w_0 = 0.3$) are shown in Figure 5c. This vibrational band is assigned as CF_3 bending mode coupled with S–N stretching mode of $[\text{NTf}_2]^-$.^{48–50} A small-frequency shift of this vibrational band by adding water has been observed: 741.4 cm^{-1} for neat $[\text{C}_2\text{MIm}][\text{NTf}_2]$ and 741.6 cm^{-1} for $[\text{C}_2\text{MIm}][\text{NTf}_2]$ –H₂O. The direction of frequency shift for the vibrational band of $[\text{NTf}_2]^-$ in $[\text{C}_2\text{MIm}][\text{NTf}_2]$ –H₂O system is the same as $[\text{BF}_4]^-$ in $[\text{C}_2\text{MIm}][\text{BF}_4]$ –H₂O system.

3.1.4. Comparison of C–H Vibrational Bands between Neat $[\text{C}_2\text{MIm}][\text{BF}_4]$ and $[\text{C}_2\text{MIm}][\text{BF}_4]$ –D₂O. Figure 6a compares the IR spectra in 550–4000 cm^{-1} for neat $[\text{C}_2\text{MIm}][\text{BF}_4]$, $[\text{C}_2\text{MIm}][\text{BF}_4]$ –H₂O, and D₂O mixtures ($w_0 = 1.0$). The purpose of this comparison is to find the water sensitivities of C(3)–H(5) stretching and C(1,2)–H(6,4) stretching modes (3125 and 3167 cm^{-1}) of the cation. (Atom labels are shown in Figure 10, vide infra.) As shown in Figure 3a,b, the edge of light water stretching bands overlaps with these cation's vibrational modes. Figure 6b shows the IR spectra in 2900–3300 cm^{-1} of neat $[\text{C}_2\text{MIm}][\text{BF}_4]$ and $[\text{C}_2\text{MIm}][\text{BF}_4]$ –D₂O ($w_0 = 1.0$). The band shapes and peak frequencies of 3125 and 3167 cm^{-1} modes are not different overall, but the intensities of 3125 and 3167 cm^{-1} modes for $[\text{C}_2\text{MIm}][\text{BF}_4]$ –D₂O are lower than those for neat $[\text{C}_2\text{MIm}][\text{BF}_4]$. The lowering of the intensities for $[\text{C}_2\text{MIm}][\text{BF}_4]$ –D₂O are due to a dilution of IL by adding D₂O. Because the spectral shifts and splitting of these modes are observed in the $[\text{C}_2\text{MIm}][\text{NTf}_2]$ –H₂O system,²⁹ the specific interaction between cation and water in $[\text{C}_n\text{MIm}][\text{BF}_4]$ –H₂O mixtures is unlikely to have happened.

3.2. Polarity. Polarities of the present IL systems have been estimated from the steady-state absorption spectrum of betaine 33. Figure 7 shows the normalized absorption spectra of betaine 33 in the series of $[\text{C}_n\text{MIm}]^+$ ($n = 2, 4, 6, 8$, and 10) based ILs with the anions of (a) $[\text{BF}_4]^-$, (b) $[\text{NTf}_2]^-$, and (c) $[\text{C}_2\text{MIm}]^+$

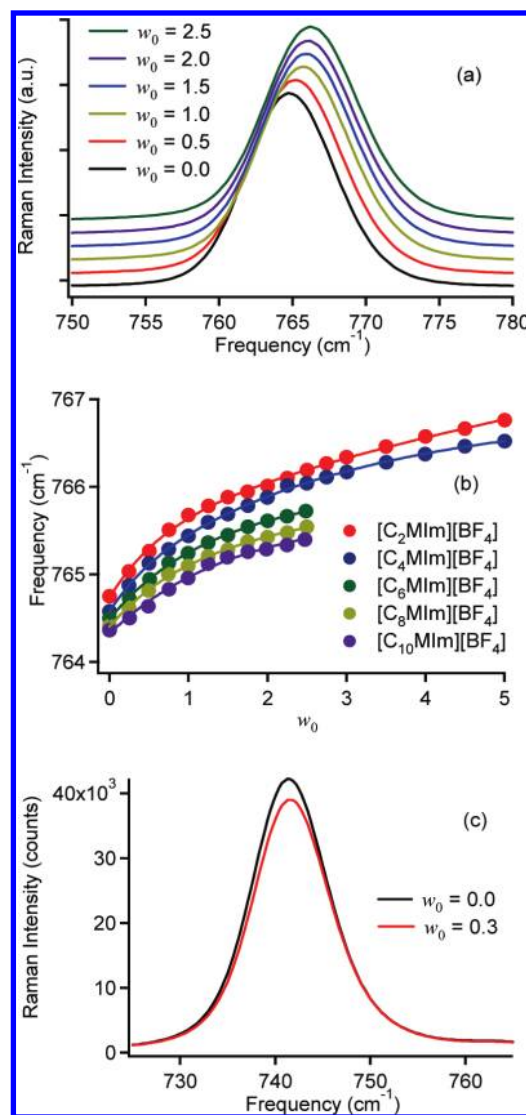


Figure 5. (a) Raman spectra of symmetric F–B stretching mode of $[\text{BF}_4]^-$ in $[\text{C}_2\text{MIm}][\text{BF}_4]$ –H₂O mixtures with $w_0 = 0.0$ (black), 0.5 (red), 1.0 (yellow), 1.5 (blue), 2.0 (purple), and 2.5 (green). (b) w_0 dependence of the frequency of symmetric F–B stretching mode of $[\text{BF}_4]^-$ in $[\text{C}_n\text{MIm}][\text{BF}_4]$ –H₂O systems. Red, blue, green, yellow, and purple denote $[\text{C}_2\text{MIm}][\text{BF}_4]$, $[\text{C}_4\text{MIm}][\text{BF}_4]$, $[\text{C}_6\text{MIm}][\text{BF}_4]$, $[\text{C}_8\text{MIm}][\text{BF}_4]$, and $[\text{C}_{10}\text{MIm}][\text{BF}_4]$ systems, respectively. (c) Raman spectra of CF_3 bending mode coupled with N–S stretching mode of $[\text{NTf}_2]^-$ in neat $[\text{C}_2\text{MIm}][\text{NTf}_2]$ (black) and $[\text{C}_2\text{MIm}][\text{NTf}_2]$ –H₂O with $w_0 = 0.3$ (red).

ILs with $[\text{BF}_4]^-$ and $[\text{NTf}_2]^-$. As displayed in Figure 7a, the absorption spectrum of betaine 33 in $[\text{C}_n\text{MIm}][\text{BF}_4]$ ILs does not really depend on the alkyl group of the cation. $[\text{C}_n\text{MIm}][\text{NTf}_2]$ ILs show a similar feature. On the other hand, there is a remarkable difference between the neat $[\text{C}_2\text{MIm}][\text{BF}_4]$ and $[\text{C}_2\text{MIm}][\text{NTf}_2]$ ILs: the absorption peak of betaine 33 in $[\text{C}_2\text{MIm}][\text{BF}_4]$ is bluer than that in $[\text{C}_2\text{MIm}][\text{NTf}_2]$ (Figure 7c). This feature has also been confirmed in the other ILs, as seen in Table 1. Table 1 also lists the values of the polarity parameters $E_T(33)$, which are estimated from the absorption maxima of betaine 33 in the ILs.⁵¹ As seen in Figure 7 and Table 1, $E_T(33)$ for the ILs with $[\text{BF}_4]^-$ is slightly larger than that for the ILs with $[\text{NTf}_2]^-$. The feature of $E_T(33)$ in the difference between $[\text{C}_n\text{MIm}][\text{BF}_4]$ and $[\text{C}_n\text{MIm}][\text{NTf}_2]$ is qualitatively identical to the results of similar polarity parameters $E_T(30)$ and E_N^{N} .⁵¹ Since a larger constituent ion generally shows the lower polarity in IL for the lower charge density arising from the larger

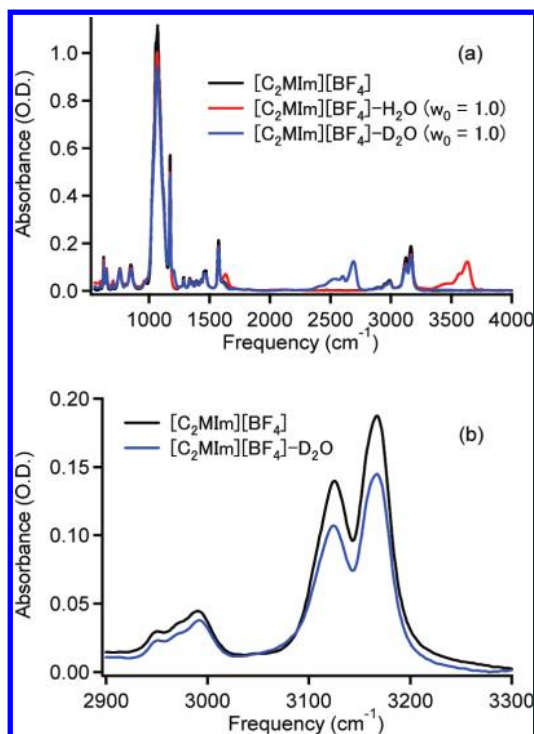


Figure 6. (a) IR spectra of neat [C₂Mim][BF₄] (black), [C₂Mim][BF₄]-H₂O mixture with $w_0 = 1.0$ (red), and [C₂Mim][BF₄]-D₂O with $w_0 = 1.0$ (blue). (b) Magnification of IR spectra (2900–3300 cm⁻¹) for neat [C₂Mim][BF₄] (black) and [C₂Mim][BF₄]-D₂O with $w_0 = 1.0$ (blue).

volume,^{52,53} the lower $E_T(33)$ value for [C_nMim][NTf₂] than [C_nMim][BF₄] seems to be due to the bigger size of [NTf₂]⁻ than [BF₄]⁻.

Figure 7d shows the normalized absorption spectra of betaine 33 in [C₂Mim][BF₄]-H₂O mixtures with $w_0 = 0, 0.25, 0.50, 1.00, 2.00$, and 3.00 . The absorption peak shifts to the short wavelength with increasing w_0 . The other IL-H₂O systems show the same tendency as well. Similar results for betaines 30 and 33 in [C₄Mim][BF₄]-H₂O systems were also reported by Sarkar and Pandey⁵⁴ and Martins et al.⁵⁵ The relationships between E_T and X_{H_2O} are not linear, but the polarity increases with adding water. Also, Sarkar and co-workers observed that the polarity probed by coumarin 153 in [C₄Mim][PF₆]-H₂O⁵⁶ and [C₆Mim][PF₆]-H₂O systems⁵⁷ increased with adding water. Figure 8 plots the water content dependences of $E_T(33)$ in the [C_nMim][BF₄]-H₂O and [C_nMim][NTf₂]-H₂O systems. As seen in Figure 8a,b, the w_0 dependence of $E_T(33)$ in both the [C_nMim][BF₄]-H₂O and [C_nMim][NTf₂]-H₂O systems is not linear. Figure 8 also plots the molar fraction of H₂O, X_{H_2O} , vs $E_T(33)$ for (c) [C_nMim][BF₄]-H₂O and (d) [C_nMim][NTf₂]-H₂O systems. If a preferential solvation of a solvatochromic dye by water molecules occurred, the relationship between the polarity parameter and water content would be nonlinear.⁵⁸ Because the relations between X_{IL} and $E_T(33)$ in the [C_nMim][BF₄]-H₂O and [C_nMim][NTf₂]-H₂O systems are almost linear, it seems that the strong preferential solvation for betaine 33 due to water molecules does not occur in the [C_nMim][BF₄]-H₂O and [C_nMim][NTf₂]-H₂O systems. Therefore, the discussion on the relationship between the vibrations and polarity is likely permitted. The similar feature was also reported in betaine 30 in aqueous methanol and acetone systems.⁵⁹

Figure 9 shows the plots of (a) $E_T(33)$ vs w_0 in EG-H₂O system with the plots of (b) peak frequencies of symmetric F-B

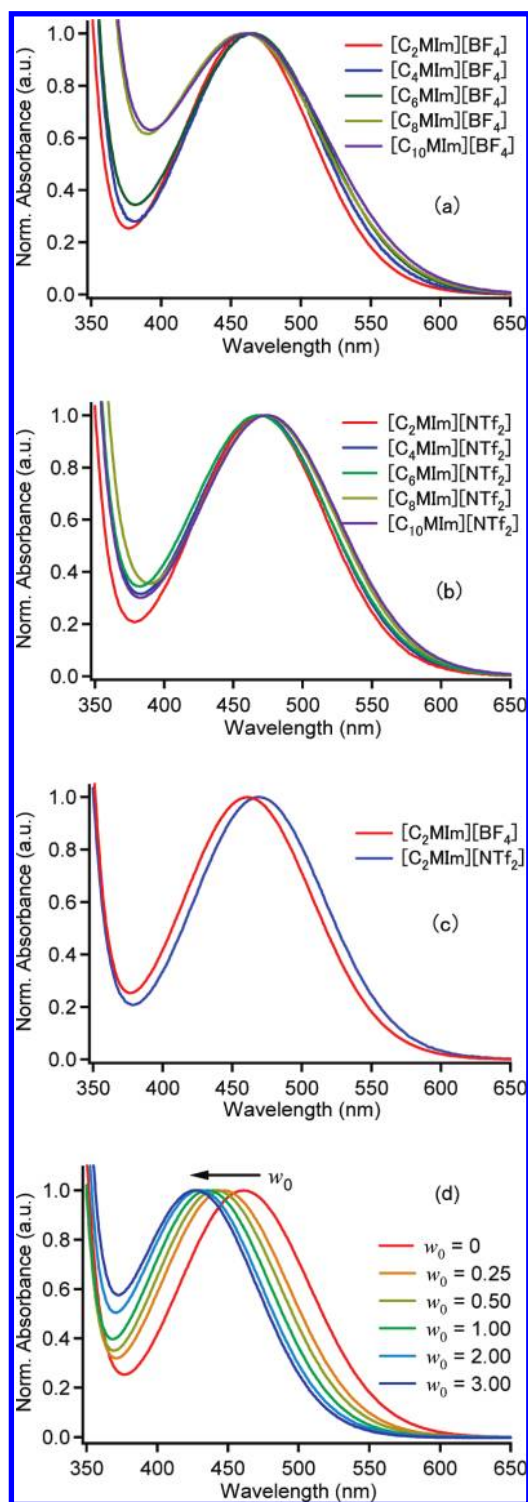


Figure 7. Absorption spectra of betaine 33 in (a) [C_nMim][BF₄] ([C₂Mim][BF₄], red; [C₄Mim][BF₄], blue; [C₆Mim][BF₄], green; [C₈Mim][BF₄], yellow; [C₁₀Mim][BF₄], purple), (b) [C_nMim][NTf₂] ([C₂Mim][NTf₂], red; [C₄Mim][NTf₂], blue; [C₆Mim][NTf₂], green; [C₈Mim][NTf₂], yellow; [C₁₀Mim][NTf₂], purple), and (c) [C₂Mim][BF₄] (red) and [C₂Mim][NTf₂] (blue). (d) w_0 dependence of the absorption spectrum of betaine 33 in [C₂Mim][BF₄]-H₂O system. Red, orange, yellow, green, light blue, and dark blue denote $w_0 = 0.00, 0.25, 0.50, 1.00, 2.00$, and 3.00 , respectively.

stretching mode of [BF₄]⁻ vs w_0 for aqueous NaBF₄ solutions and (c) peak frequencies of symmetric F-B stretching mode of [BF₄]⁻ vs $E_T(33)$ for aqueous Na[BF₄] solutions and peak frequencies of CF₃ bending mode coupled with S-N stretching mode of [NTf₂]⁻ vs $E_T(33)$ for aqueous Li[NTf₂] solutions. As

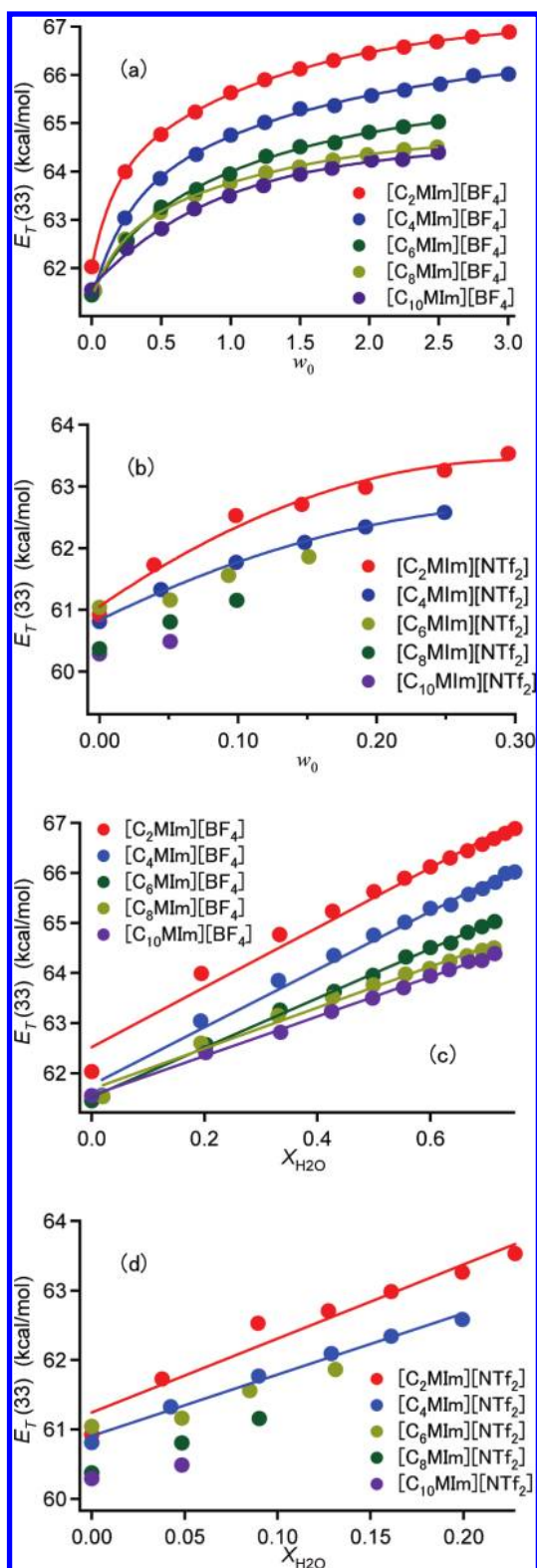


Figure 8. w_0 dependence of $E_T(33)$ in (a) $[C_n\text{Mim}][\text{BF}_4]$ -H₂O and (b) $[C_n\text{Mim}][\text{NTf}_2]$ -H₂O systems and $X_{\text{H}_2\text{O}}$ dependence of $E_T(33)$ in (a) $[C_n\text{Mim}][\text{BF}_4]$ -H₂O and (b) $[C_n\text{Mim}][\text{NTf}_2]$ -H₂O systems. ($[C_2\text{Mim}]$ ILs, red; $[C_4\text{Mim}]$ ILs, blue; $[C_6\text{Mim}]$ ILs, green; $[C_8\text{Mim}]$ ILs, yellow; $[C_{10}\text{Mim}]$ ILs, purple.)

well as IL-H₂O systems, $E_T(33)$ in EG-H₂O system increases with increase in w_0 .

3.3. Refractive Index and Water Saturation. As shown in Table 1, the refractive indices of the ILs become slightly larger with the longer alkyl group of cation. The refractive indices of the $[C_n\text{Mim}][\text{BF}_4]$ ILs are smaller than that of $[C_n\text{Mim}][\text{NTf}_2]$

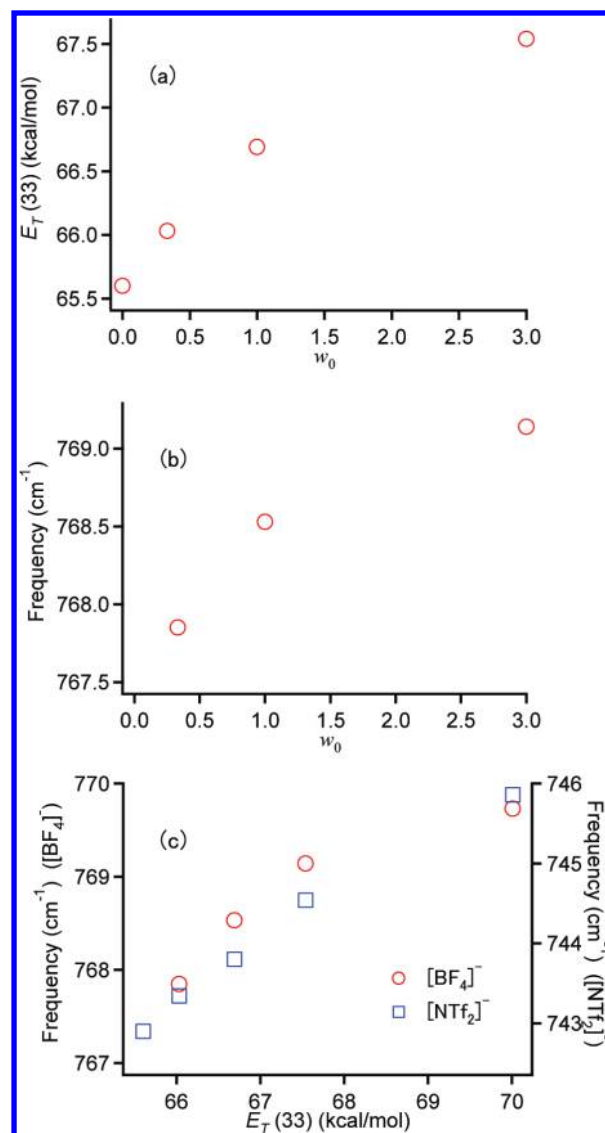


Figure 9. Plots of (a) of $E_T(33)$ vs w_0 for EG-H₂O system, (b) frequency of symmetric F-B stretching mode of $[\text{BF}_4]^-$ vs w_0 for Na[BF₄] in EG-H₂O, and (c) frequency of symmetric F-B stretching mode of $[\text{BF}_4]^-$ and CF₃ bending mode coupled with N-S stretching mode of $[\text{NTf}_2]^-$ vs $E_T(33)$ in EG-H₂O solutions of Na[BF₄] and Li[NTf₂].

ILs when a comparison is made for the cations with the same alkyl group. The difference in refractive index between $[C_n\text{Mim}][\text{BF}_4]$ and $[C_n\text{Mim}][\text{NTf}_2]$ is due to the differences in polarizability and density (or ionic volume), because the larger polarizability and larger ionic volume of $[\text{NTf}_2]^-$ than $[\text{BF}_4]^-$ provide a larger refractive index.

Water saturation values S_w of the ILs are summarized in Table 1. The water saturations of both the $[C_n\text{Mim}][\text{BF}_4]$ and $[C_n\text{Mim}][\text{NTf}_2]$ systems become larger with the longer alkyl group of cation. We also notice that $[C_{n=2,4}\text{Mim}][\text{BF}_4]$ ILs mix homogeneously with water in the entire concentration range, while $[C_{n=6,8,10}\text{Mim}][\text{BF}_4]$ ILs show water saturations at certain water contents. Since the hydrophobicity increases with the longer alkyl group,⁶⁰ the observed trend of water saturation in the ILs is reasonable. In Table 1, the rescaled values $w_{0\text{sw}}$, which is defined as the molar concentration ratio between IL and water at water saturation, are also summarized to see the molar ratio between water and IL. It is clear that $[C_n\text{Mim}][\text{NTf}_2]$ ILs are more hydrophobic than $[C_n\text{Mim}][\text{BF}_4]$ ILs. $[\text{NTf}_2]^-$ shows a strong amphiphilic nature on the basis of the separative scales

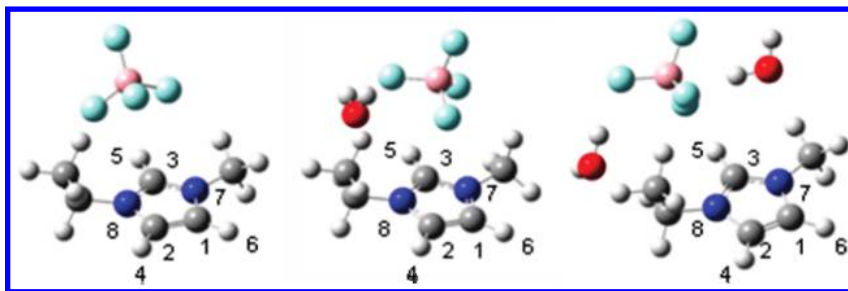


Figure 10. Optimized structures of [C₂Mim][BF₄], [C₂Mim][BF₄]-H₂O, and [C₂Mim][BF₄]-2H₂O clusters by ab initio quantum chemistry calculations based on the B3LYP/6-311+G(d,p) level of theory.

TABLE 2: Some Vibrational Modes and Frequencies of Optimized [C₂Mim][BF₄], [C₂Mim][BF₄]-H₂O, and [C₂Mim][BF₄]-2H₂O Clusters and Experimentally Observed Vibrational Spectra for Neat [C₂Mim][BF₄] and [C₂Mim][BF₄]-H₂O or D₂O ($w_0 = 1.0$)^a

vibrational mode	calculation (cm ⁻¹)			experiment (cm ⁻¹)	
	[C ₂ Mim][BF ₄]	[C ₂ Mim][BF ₄]-H ₂ O	[C ₂ Mim][BF ₄]-2H ₂ O	[C ₂ Mim][BF ₄]	[C ₂ Mim][BF ₄]-H ₂ O (D ₂ O) ^b
B-F stretch (sym)	735.6	740.2	736.8	764.6	765.7
C(3)-H(5) stretch ^c	3259.0	3215.0	3196.9	3125.2	3124.3
C(1,2)-H(6,4) stretches (asym) ^c	3276.9	3278.8	3274.6	3166.9 ^d	3166.7 ^d
C(1,2)-H(6,4) stretches (sym) ^c	3295.4	3297.3	3293.1	3166.9 ^d	3166.7 ^d

^a The level of theory for the calculations is B3LYP/6-311+G(d,p). ^b B-F stretch is for [C₂Mim][BF₄]-H₂O and C-H stretches are for [C₂Mim][BF₄]-D₂O. ^c Identifications of X(n) are shown in Figure 10. ^d Asymmetric and symmetric C-H stretching modes in measured IR spectra are overlapped. See Figure 3.

of relative hydrophobicity and hydrophilicity.⁶¹ For simplicity, however, we consider the simple single scale for the hydrophobicity/hydrophilicity based on the water saturation in this study, as well as previous studies.^{1,35,62}

3.4. Ab Initio Quantum Chemistry Calculation. Figure 10 shows the optimized structures of the clusters of [C₂Mim][BF₄], [C₂Mim][BF₄]-H₂O, and [C₂Mim][BF₄]-2H₂O. The result indicates that H₂O affects the distance and position between [C₂Mim]⁺ and [BF₄]⁻. Some vibrational frequencies of normal modes of the clusters are summarized in Table 2. The frequencies of the normal modes are not rescaled for simplicity, though the values can be scaled.⁶³ C(3)-H(5) stretching mode shifts to the low-frequency side by the existence of H₂O (Table 2). The other vibrational modes are little affected by H₂O. This result indicates that the frequencies of the vibrational modes of the ions are rather insensitive to water molecules, except for the C(3)-H(5) stretching mode.

4. Discussion

4.1. Microenvironment of Ions. As shown in Figure 5a, symmetric F-B stretching mode of [BF₄]⁻ in the [C_nMim][BF₄]-H₂O shifts to high frequency with increase in w_0 . Most of the vibrational modes of molecules are influenced by hydrogen bonds of solvents.⁶⁴ Recent study by Danten et al. showed that water molecules were stabilized in a symmetric structure interacting with two [BF₄]⁻ anions at a very low water concentration.²⁸ Though the water content range is small compared to the [C_nMim][BF₄]-H₂O systems, the frequency of the vibrational mode of [NTf₂]⁻ in the [C_nMim][NTf₂]-H₂O systems becomes high by adding water (Figure 5c). Therefore, it is plausible that the interaction between water and anion provides the frequency shifts of the anions' vibrational modes in the ILs. In general, there are two possible origins for the water sensitivities of the anions' vibrational modes. One is microstructure and the other is micropolarity. Surely, the micropolarity depends on the microstructure. Here, the micropolarity is the betaine 33 perspective.

Let us discuss the microstructure first. Because of the two distinct parts (hydrophobic and ionic parts) of [C_nMim]⁺, particularly for one having a long alkyl group, even neat ILs are rather inhomogeneous in the microscopic viewpoint. Recent dielectric relaxation and polarizability anisotropy relaxation results suggested evidence of mesoscopic aggregation in ILs whose cation has a short ethyl group.⁶⁵ Some X-ray diffraction^{66,67} and MD simulation studies⁶⁸⁻⁷⁰ also showed that the microsegregation in ILs became more pronounced with the longer alkyl group of the imidazolium cation. Since the volume fraction of the hydrophilic (or ionic) part, which interacts with water molecules, in IL depends strongly on the alkyl group of imidazolium cation, the microstructure in IL-H₂O is likely influenced by the alkyl group of the cation. However, the change in the w_0 dependence of the frequency of the anion's vibrational mode with the different cation is rather monotonic, except for the amplitude of the frequency shift, as shown in Figure 5b. Therefore, the effect of microsegregation size on the vibrational mode of anion is probably minor. This consideration is also supported by the quantum chemistry calculation result except for the C(3)-H(5) mode (Table 2).

Next, we consider the micropolarity. The polarity in the mixtures increases with increasing w_0 , as shown in Figure 8a,b. This trend is not surprising, because water is more polar than the ILs. On the other hand, the w_0 dependence of $E_T(33)$ is not linear for all the IL systems. This feature is somewhat similar to that in the vibrational modes of [BF₄]⁻ and [NTf₂]⁻ anions (Figure 5). To understand the correlation between the polarity and the frequencies of the vibrational bands of the anions, we have examined the EG-H₂O system. The polarity in the EG-H₂O system increases with increasing w_0 (Figure 9a). Correlating with the polarity, the frequency of the vibrational band of [BF₄]⁻ for Na[BF₄] in the EG-H₂O system shifts to the higher frequency with larger w_0 in the mixtures as shown in Figure 9b. Though we do not show the data of the vibrational band of [NTf₂]⁻ for Li[NTf₂] in EG-H₂O system, the same tendency was observed. Figure 9c shows that the frequencies

of the vibrational bands of $[\text{BF}_4]^-$ and $[\text{NTf}_2]^-$ in EG–H₂O mixtures becomes high with increase in $E_T(33)$, and the correlations are not very far from a linear relation. Since aqueous alcohols such as methanol and ethanol show microsegregations,⁷¹ it could also be expected in EG–H₂O mixtures. However, the probe molecule, betaine 33, is rather large, and thus, the structural information for the smaller segregation (or smaller clustering) could be less sensitive, and that for the larger segregation (or larger clustering) is more pronounced for the betaine 33 probe. Surely, the polarity includes the information on the microstructure, but the sensitivity to the structural information for the betaine 33 depends strongly on the segregation size. Consequently, the result of $\text{Na}[\text{BF}_4]$ and $\text{Li}[\text{NTf}_2]$ in EG–H₂O largely reflects the polarity, and we conclude that the observed w_0 dependence of the vibrational modes of the anions in the IL–H₂O systems comes mainly from the polarity based on the betaine perspective.

Additional noticeable evidence for the w_0 dependence of the B–F stretching mode and $E_T(33)$ in the IL–H₂O systems is the alkyl-group dependence of the cation (Figure 8). The feature of alkyl-group dependence of the plots of w_0 values vs B–F stretching mode frequency is similar to that of the plots of w_0 vs $E_T(33)$. Since the volume fraction of the hydrophobic part becomes larger for the cation with a longer alkyl group, water cannot completely cover a large polarity probe molecule and anions for the large hydrophobic region due to the longer alkyl group. Thus, the polarity mildly changes for the cation with the longer alkyl group compared to the cation having the shorter alkyl group.

4.2. Microenvironment of Water. As displayed in Figures 3 and 4, two clear bands are observed at ca. 3560 and 3640 cm^{-1} in the low water content region ($w_0 < 0.5$), and the two broad bands at ca. 3250 and 3450 cm^{-1} are pronounced by increasing water content ($w_0 > 0.5$). Namely, water molecules make a less structured hydrogen-bonding network at the low water content region than at the high water content region (Figure 3d). However, if we carefully view the figures, the $[\text{C}_n\text{Mim}][\text{BF}_4]$ –H₂O with $w_0 = 0.5$ and $[\text{C}_2\text{Mim}][\text{NTf}_2]$ –H₂O with $w_0 = 0.3$ already exist as a liquid like water. This fact indicates that water molecules in the ILs localize even in low water concentration.

As shown in Figure 3d, the w_0 dependence of the relative area of the vibrational bands of the stretching modes for isolated and bulk water in the $[\text{C}_n\text{Mim}][\text{BF}_4]$ –H₂O systems does not really vary among the $[\text{C}_{n=6,8,10}\text{Mim}][\text{BF}_4]$ ILs. This shows that the water aggregation states do not differ among the ILs. If we take the hydrophobicity of the alkyl group into consideration, the water aggregation state in ILs should depend strongly on the alkyl group of the cations. This feature of the alkyl-group dependence of the cation in water aggregation may be due to the structure of the ILs. Because water interacts preferentially with the ionic part in IL, water should locate dominantly at the ionic parts. The slight difference in the low w_0 region ($w_0 < 0.2$) for the $[\text{C}_{n=2,4}\text{Mim}][\text{BF}_4]$ systems from the $[\text{C}_{n=6,8,10}\text{Mim}][\text{BF}_4]$ systems suggests that the segregation is more pronounced in the $[\text{C}_{n=6,8,10}\text{Mim}][\text{BF}_4]$ ILs than the $[\text{C}_{n=2,4}\text{Mim}][\text{BF}_4]$ ILs. However, the high water content region shows the similar feature in all the $[\text{C}_n\text{Mim}][\text{BF}_4]$ ILs. Polarity in the neat ILs is rather independent of the alkyl group of the cation (Figure 7 and Table 1). In contrast, the polarity depends dramatically on the alkyl group in typical molecular liquids such as alcohols.^{72,73} As well as the polarity, the segregation structure also shows similar features.⁷⁴ These facts mean that the ionic part in ILs significantly affects the polarity compared with the

hydroxyl group in alcohols. Thus, the microscopic structure of water is mainly governed by the nature of the ionic part in ILs and is little affected by the hydrophobic part in ILs. Because the water localization at ionic parts in IL critically weakens the interionic interaction, some physical properties such as shear viscosity and surface tension are largely affected by the existence of water. A study on the interionic/intermolecular vibrational band, which is directly influenced by the microscopic interionic/intermolecular interaction, in IL–H₂O systems is warranted for a further physical insight.

5. Conclusions

We have investigated the microscopic perspectives in $[\text{C}_n\text{Mim}][\text{BF}_4]$ –H₂O and $[\text{C}_n\text{Mim}][\text{NTf}_2]$ –H₂O systems by Raman and IR spectroscopies and a solvatochromic probe betaine 33 in this study. Water structure does not really change among the ILs with different alkyl groups of cation. This result indicates that the water aggregation state in the ILs is mainly determined by the ionic property in the ILs and is little influenced by the hydrophobicity of the ILs. On the other hand, the frequencies of the vibrational bands of $[\text{BF}_4]^-$ and $[\text{NTf}_2]^-$ in the ILs depend on the water content. From the comparison of the observation of the vibrational spectroscopic experiment with the results of the quantum chemistry calculation and polarity measurement, it becomes clear that the frequency shifts of the vibrational bands of $[\text{BF}_4]^-$ and $[\text{NTf}_2]^-$ are mainly due to the polarity change. We have also found that the magnitude of frequency shift of the vibrational bands of $[\text{BF}_4]^-$ and $[\text{NTf}_2]^-$ in the IL–H₂O systems is smaller with the longer alkyl group of the imidazolium cation for the lower polarity of the longer alkyl group.

Acknowledgment. We thank Dr. Tomotsumi Fujisawa (Chiba University) for fruitful discussion and proofreading of this manuscript. This study was partially supported by MEXT of Japan (Grant-in-Aids for Young Scientists (A): 21685001 (HS) and Priority Area “Science of Ionic Liquids”: 17073002 (KN)). This work was also supported in part by the Futaba Electronics Memorial Foundation (HS).

Supporting Information Available: Details of the synthesis procedures of respective ILs, quantum chemistry calculation results (atom coordinates), spectrum of the fluorescent light used in refractive index measurement, and full author list of ref 41 are summarized. This material is available free of charge via the Internet at <http://pubs.acs.org>.

References and Notes

- (1) *Ionic Liquids in Synthesis*, 2nd ed.; Wasserscheid, P., Welton, T., Eds.; Wiley-VCH: Weinheim, 2008.
- (2) *Electrochemical Aspects of Ionic Liquids*; Ohno, H., Ed.; Wiley-Interscience: Hoboken, 2005.
- (3) *Acc. Chem. Res.: Special Issue on Ionic Liquids*, Rogers, R. D.; Voth, G. A., Eds.; **2007**; Vol. 40.
- (4) *J. Phys. Chem. B: Special Issue on Physical Chemistry of Ionic Liquids*, Wishart, J. F.; Castner, E. W., Jr., Eds.; **2007**; Vol. 111.
- (5) Wishart, J. F. *Energy Environ. Sci.* **2009**, 2, 967.
- (6) Plechkova, N. V.; Seddon, K. R. *Chem. Soc. Rev.* **2008**, 37, 123.
- (7) Weingaertner, H. *Angew. Chem., Int. Ed. Engl.* **2008**, 47, 654.
- (8) Ohno, H.; Fukumoto, K. *Electrochemistry* **2008**, 76, 16.
- (9) Parvulescu, V. I.; Hardacre, C. *Chem. Rev.* **2007**, 107, 2615.
- (10) Deetlefs, M.; Seddon, K. R. *Chem. Today* **2006**, 24, 16.
- (11) Huddleston, J. G.; Visser, A. E.; Reichert, W. M.; Willauer, H. D.; Broker, G. A.; Rogers, R. D. *Green Chem.* **2001**, 3, 156.
- (12) Widegren, J. A.; Laesecke, A.; Magee, J. W. *Chem. Commun.* **2005**, 1610.
- (13) Gomez, E.; Gonzalez, B.; Dominguez, A.; Tojo, E.; Tojo, J. *J. Chem. Eng. Data* **2006**, 51, 696.

- (14) Yang, J.-Z.; Tong, J.; Li, J.-B.; Li, J.-G.; Tong, J. *J. Colloid Interface Sci.* **2007**, *313*, 374.
- (15) Freire, M. G.; Carvalho, P. J.; Fernandes, A. M.; Marrucho, I. M.; Queimada, A. J.; Coutinho, J. A. P. *J. Colloid Interface Sci.* **2007**, *314*, 621.
- (16) Kanakubo, M.; Umecky, T.; Aizawa, T.; Kurata, Y. *Chem. Lett.* **2005**, *34*, 324.
- (17) Castner, E. W., Jr.; Wishart, J. F.; Shirota, H. *Acc. Chem. Res.* **2007**, *40*, 1217.
- (18) Iwata, K.; Okajima, H.; Saha, S.; Hamaguchi, H.-O. *Acc. Chem. Res.* **2007**, *40*, 1174.
- (19) Hyun, B. R.; Dzyuba, S. V.; Bartsch, R. A.; Quitevis, E. L. *J. Phys. Chem. A* **2002**, *106*, 7579.
- (20) Giraud, G.; Gordon, C. M.; Dunkin, I. R.; Wynne, K. *J. Chem. Phys.* **2003**, *119*, 464.
- (21) Shirota, H.; Funston, A. M.; Wishart, J. F.; Castner, E. W., Jr. *J. Chem. Phys.* **2005**, *122*, 184512.
- (22) Fujisawa, T.; Nishikawa, K.; Shirota, H. *J. Chem. Phys.* **2009**, *131*, 244519.
- (23) Hayashi, S.; Ozawa, R.; Hamaguchi, H. *Chem. Lett.* **2003**, *32*, 498.
- (24) Umebayashi, Y.; Fujimori, T.; Sukizaki, T.; Asada, M.; Fujii, K.; Kanzaki, R.; Ishiguro, S.-i. *J. Phys. Chem. A* **2005**, *109*, 8976.
- (25) Cammarata, L.; Kazarian, S. G.; Salter, P. A.; Welton, T. *Phys. Chem. Chem. Phys.* **2001**, *3*, 5192.
- (26) Jeon, Y.; Sung, J.; Kim, D.; Seo, C.; Cheong, H.; Ouchi, Y.; Ozawa, R.; Hamaguchi, H.-o. *J. Phys. Chem. B* **2008**, *112*, 923.
- (27) Jeon, Y.; Sung, J.; Seo, C.; Lim, H.; Cheong, H.; Kang, M.; Moon, B.; Ouchi, Y.; Kim, D. *J. Phys. Chem. B* **2008**, *112*, 4735.
- (28) Danten, Y.; Cabao, M. I.; Besnard, M. *J. Phys. Chem. A* **2009**, *113*, 2873.
- (29) Umebayashi, Y.; Jiang, J.-C.; Shan, Y.-L.; Lin, K.-H.; Fujii, K.; Seki, S.; Ishiguro, S.-I.; Lin, S. H.; Chang, H.-C. *J. Chem. Phys.* **2009**, *130*, 124503.
- (30) Koddermann, T.; Christiane, Wertz; Heintz, A.; Ludwig, R. *Angew. Chem., Int. Ed. Engl.* **2006**, *45*, 3697.
- (31) Sando, G. M.; Dahl, K.; Owrutsky, J. C. *J. Phys. Chem. B* **2007**, *111*, 4901.
- (32) Koeborg, M.; Wu, C.-C.; Kim, D.; Bonn, M. *Chem. Phys. Lett.* **2007**, *439*, 60.
- (33) Seddon, K. R.; Stark, A.; Torres, M. J. *ACS Symp. Ser.* **2002**, *819*, 34.
- (34) Holbrey, J. D.; Seddon, K. R. *J. Chem. Soc., Dalton Trans.* **1999**, 2133.
- (35) Bonhote, P.; Dias, A. P.; Papageorgiou, N.; Kalyanasundaram, K.; Gratzel, M. *Inorg. Chem.* **1996**, *35*, 1168.
- (36) Huddleston, J. G.; Willauer, H. D.; Swatoski, R. P.; Visser, A. E.; Rogers, R. D. *Chem. Commun.* **1998**, 1765.
- (37) Dzyuba, S. V.; Bartsch, R. A. *J. Heterocycl. Chem.* **2001**, *38*, 265.
- (38) *CRC Handbook of Chemistry and Physics*; 89 ed.; Lide, D. R., Ed.; CRC Press: Boca Raton, 2008.
- (39) Becke, A. D. *J. Chem. Phys.* **1993**, *98*, 5648.
- (40) Lee, C.; Yang, W.; Parr, R. G. *Phys. Rev. B* **1988**, *37*, 785.
- (41) Frisch, M. J.; Trucks, G. W.; Schlegel, H. B.; Scuseria, G. E.; Robb, M. A.; Cheeseman, J. R.; Montgomery, J. A., Jr.; Vreven, T.; Kudin, K. N.; Burant, J. C.; et al. *Gaussian 03*; Gaussian, Inc.: Pittsburgh, PA, 2003.
- (42) Eisenberg, D.; Kauzmann, W. *The Structure and Properties of Water*; Oxford University Press: New York, 1969.
- (43) Walrafen, G. E.; Hokmabadi, M. S.; Yangt, W.-H. *J. Phys. Chem.* **1988**, *92*, 2433.
- (44) Moule, D. C. *Can. J. Chem.* **1966**, *44*, 3009.
- (45) Conrad, M. P.; Strauss, H. L. *J. Phys. Chem.* **1987**, *91*, 1668.
- (46) Luck, W. A. P. *Angew. Chem., Int. Ed. Engl.* **1980**, *19*, 28.
- (47) Onori, G.; Santucci, A. *J. Phys. Chem.* **1993**, *97*, 5430.
- (48) Bakker, A.; Gejji, S.; Lindgren, J.; Hermansson, K.; Probst, M. M. *Polymer* **1995**, *36*, 4371.
- (49) Rey, I.; Johansson, P.; Lindgren, J.; Lassegues, J. C.; Grondin, J.; Servant, L. *J. Phys. Chem. A* **1998**, *102*, 3249.
- (50) Umebayashi, Y.; Mitsugi, T.; Fukuda, S.; Fujimori, T.; Fujii, K.; Kanzaki, R.; Takeuchi, M.; Ishiguro, S.-I. *J. Phys. Chem. B* **2007**, *111*, 13028.
- (51) Reichardt, C. *Green Chem.* **2005**, *7*, 339.
- (52) Kimura, Y.; Hamamoto, T.; Terashima, M. *J. Phys. Chem. A* **2007**, *111*, 7081.
- (53) Kobrak, M. N. *Green Chem.* **2008**, *10*, 80.
- (54) Sarkar, A.; Pandey, S. *J. Chem. Eng. Data* **2006**, *51*, 2051.
- (55) Martins, C. T.; Sato, B. M.; Seoud, O. A. E. *J. Phys. Chem. B* **2008**, *112*, 8330.
- (56) Chakrabarty, D.; Chakraborty, A.; Seth, D.; Hazra, P.; Sarkar, N. *Chem. Phys. Lett.* **2004**, *397*, 469.
- (57) Chakrabarty, D.; Chakraborty, A.; Seth, D.; Sarkar, N. *J. Phys. Chem. A* **2005**, *109*, 1764.
- (58) Shirota, H.; Castner, E. W., Jr. *J. Chem. Phys.* **2000**, *112*, 2367.
- (59) Shirota, H.; Ohkawa, K.; Kuwabara, N.; Endo, N.; Horie, K. *Macromol. Chem. Phys.* **2000**, *201*, 2210.
- (60) Israelachvili, J. N. *Intermolecular and Surface Forces*, 2nd ed.; Academic Press: London, 1992.
- (61) Kato, H.; Nishikawa, K.; Koga, Y. *J. Phys. Chem. B* **2008**, *112*, 2655.
- (62) Seddon, K. R.; Stark, A.; Torres, M. J. *Pure Appl. Chem.* **2000**, *72*, 2275.
- (63) Andersson, M. P.; Uvdal, P. *J. Phys. Chem. A* **2005**, *109*, 2937.
- (64) Hobza, P.; Havlas, Z. *Chem. Rev.* **2000**, *100*, 4253.
- (65) Turton, D. A.; Hunger, J.; Stoppa, A.; Hefter, G.; Thoman, A.; Walther, M.; Buchner, R.; Wynne, K. *J. Am. Chem. Soc.* **2009**, *131*, 11140.
- (66) Triolo, A.; Russina, O.; Bleif, H.-J.; Di Cola, E. *J. Phys. Chem. B* **2007**, *111*, 4641.
- (67) Xiao, D.; Larry, G.; Hines, J.; Li, S.; Bartsch, R. A.; Quitevis, E. L.; Russina, O.; Triolo, A. *J. Phys. Chem. B* **2009**, *113*, 6426.
- (68) Wang, Y.; Voth, G. A. *J. Am. Chem. Soc.* **2005**, *127*, 12192.
- (69) Wang, Y.; Voth, G. A. *J. Phys. Chem. B* **2006**, *110*, 18601.
- (70) Wang, Y.; Jiang, W.; Yan, T.; Voth, G. A. *Acc. Chem. Res.* **2007**, *40*, 1193.
- (71) Dixit, S.; Crain, J.; Poon, W. C. K.; Finney, J. L.; Soper, A. K. *Nature* **2002**, *416*, 829.
- (72) Reichardt, C. *Chem. Rev.* **1994**, *94*, 2319.
- (73) Horng, M. L.; Gardecki, J. A.; Papazyan, A.; Maroncelli, M. *J. Phys. Chem.* **1995**, *99*, 17311.
- (74) Triolo, A.; Russina, O.; Fazio, B.; Triolo, R.; Cola, E. D. *Chem. Phys. Lett.* **2008**, *457*, 362.